

A New Class of Near-Infrared Electrochromic Oxamide-Based Dinuclear Ruthenium Complexes

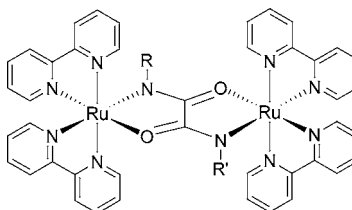
Majid F. Rastegar, Erin K. Todd, Hongding Tang, and Zhi Yuan Wang*

Department of Chemistry, Carleton University, 1125 Colonel By Drive, Ottawa, Ontario, Canada K1S 5B6

wang@ccs.carleton.ca

Received September 28, 2004

ABSTRACT



We report the synthesis of a new class of symmetric and unsymmetric oxamide-based dinuclear ruthenium complexes. These complexes were characterized by NMR, ESI-MS, and electrochemical methods. Spectroelectrochemical analysis of the complexes showed broad absorptions in the NIR region for the mixed-valence state of the complexes. The introduction of a chiral group into the bridging ligand produced an optically active complex that was studied using circular dichroism.

Homo- and heteropolynuclear metal complexes are of interest for studying the electron-transfer phenomena¹ and for applications in molecular electronics,² solar cells,³ and as optical attenuators.⁴ Ruthenium complexes containing bipyridine ligands have attracted a great deal of interest in light of their interesting luminescent and electrochemical properties. The work by Kaim et al. showed that dinuclear ruthenium complexes with 1,2-dicarbonylhydrazido (DCH) ligands (Figure 1) are highly electrochromic.⁵ DCH–Ru complexes

in the mixed-valence state ($\text{Ru}^{\text{II}}/\text{Ru}^{\text{III}}$) display intense near-infrared (NIR) absorptions between 1000 and 2000 nm due to intervalence charge transfer (IVCT) transitions between the two metallic nuclei. The $\text{Ru}^{\text{II}}/\text{Ru}^{\text{II}}$ state does not show any absorption in the NIR region, while the $\text{Ru}^{\text{III}}/\text{Ru}^{\text{III}}$ state exhibits an absorption at around 800 nm. Extensive studies on dinuclear ruthenium complexes with DCH bridging ligands have been carried out in our group in the past few years.^{4,6} Several synthetic routes to various ligands have been established, and a series of DCH–Ru complexes having

(1) (a) Creutz, C.; Taube, H. *J. Am. Chem. Soc.* **1969**, *91*, 3988. (b) Taube, H. *Angew. Chem.* **1984**, *96*, 315. (c) Taube, H. *Angew. Chem.* **1984**, *96*, 329.

(2) Mikkelsen, K. V.; Ranter, M. A. *Chem. Rev.* **1987**, *87*, 113.

(3) (a) Subramanian, V.; Evans, D. G. *J. Phys. Chem.* **2004**, *108*, 1085.

(b) Marin, V.; Holder, E.; Schubert, U. S. *J. Polym. Sci., Part A: Polym. Chem.* **2004**, *42*, 374.

(4) (a) Qi, Y.; Desjardins, P.; Wang, Z. Y. *J. Opt. A: Pure Appl. Opt.* **2002**, *4*, S273. (b) Qi, Y.; Desjardins, P.; Meng, X. S.; Wang, Z. Y. *Opt. Mater.* **2003**, *21*, 255. (c) Qi, Y.; Wang, Z. Y. *Macromolecules* **2003**, *36*, 3146. (d) Wang, Z. Y.; Zhang, J.; Wu, X.; Birau, M.; Yu, G.; Yu, H.; Qi, Y.; Desjardins, P.; Meng, X. S.; Gao, J. P.; Todd, E.; Song, N. H.; Bai, Y. W.; Beaudin, A. M. R.; LeClair, G. *Pure Appl. Chem.* **2004**, *76*, 1435.

(5) (a) Kasack, V.; Kaim, W.; Binder, H.; Jordanov, J.; Roth, E. *Inorg. Chem.* **1995**, *34*, 1924. (b) Kaim, W.; Kasack, V.; Binder, H.; Roth, E.; Jordanov, J. *J. Angew. Chem., Int. Ed. Engl.* **1988**, *27*, 1174. (c) Kaim, W.; Kasack, V. *Inorg. Chem.* **1990**, *29*, 4696.

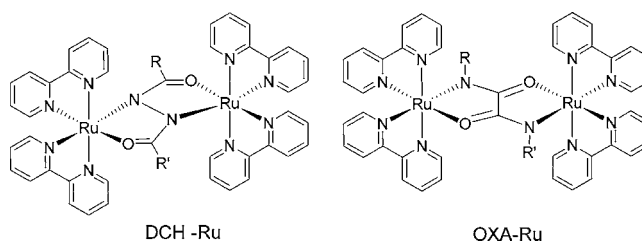
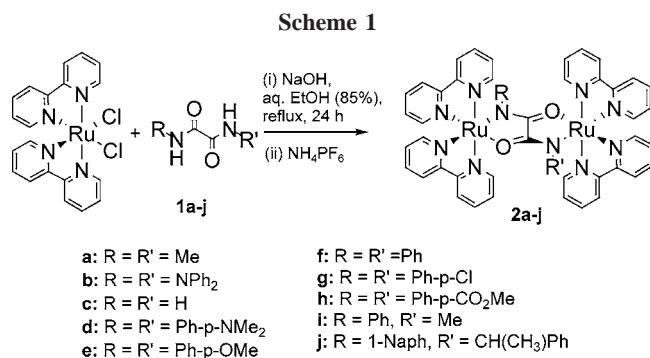


Figure 1. DCH–Ru and OXA–Ru complexes.



various donor and acceptor groups have been synthesized. In addition, linear and cross-linked polymers containing the DCH–Ru moieties have been prepared.

DCH and OXA ligands contain the CO–N–N–CO and N–CO–CO–N moieties, respectively, and are structural isomers. Accordingly, the ruthenium complexes based on the OXA ligand or OXA–Ru complexes as shown in Figure 1, should be considered as isomers to DCH–Ru complexes. Since DCH and OXA ligands can be synthesized in a number of different ways and can have different functional groups for further manipulation, it is necessary to have access to the OXA–Ru complexes for studying and comparing the electrical and optical properties for potential applications. However, surprisingly enough, OXA–Ru complexes have not been reported and are still unknown in the literature to date. We report herein the synthesis and characterization of a new class of dinuclear ruthenium complexes based on the oxamide ligands.

For DCH–Ru complexes, the NIR absorption depends on the electronic environment of the two metal cations, which is strongly influenced by the substituents on the ligands. Changing the electron-withdrawing or electron-donating ability of the ligands will affect the HOMO/LUMO energy levels and thus cause changes in the NIR λ_{max} values. Accordingly, a series of OXA–Ru complexes containing electron-donating and electron-withdrawing groups on the oxamide nitrogen atoms were prepared (Scheme 1).

The symmetric ligands (**1a–h**) were synthesized by reaction of oxalyl chloride with the corresponding amines. Unsymmetric ligands **1i** and **1j** were prepared in two steps, first by refluxing aniline or 1-naphthylamine in diethyl oxalate to give monosubstituted compounds that were subsequently reacted with methylamine and (*S*)-(-)- α -methylbenzylamine, respectively. In all cases, the ligands were isolated in yields greater than 80%. To make complexes **2a–j**, a mixture of ruthenium bis(bipyridine)dichloride and the corresponding ligands were heated to reflux in the presence of base under a nitrogen atmosphere. The purple complexes were isolated upon addition of ammonium hexafluorophosphate and then passed through an alumina-gel column (eluted with a mixture of acetonitrile and toluene, 1:1 v/v), which

(6) Qi, Y.; Desjardins, P.; Birau, M.; Wu, X.; Wang, Z. Y. *Chin. J. Polym. Sci.* **2003**, *21*, 147.

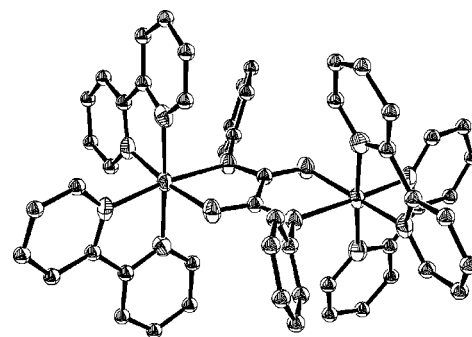


Figure 2. ORTEP structure of **2f**.

allowed for the isolation of pure OXA–Ru complexes in their Ru^{II}/Ru^{II} state.

Figure 2 shows the ORTEP crystal structure of complex **2f** (as one of the stereoisomers).⁷ The crystals were grown by dissolving **2f** in acetone and slow evaporation of the solvent at room temperature. The C–N–C_{ph}–C_{ph} torsion angle is 69.2°, showing the weak resonance effect. Two fused five-membered cyclic rings are planar, similar to the DCH–Ru series.⁵ There is also π – π interaction between the bipyridine groups within the unit cell.

Studies on the stereochemistry of mononuclear⁸ and dinuclear ruthenium⁹ complexes have attracted much interest in the area of supramolecular chemistry. In dinuclear ruthenium complexes, the metal centers can possess right- or left-handed chirality (Δ or Λ), respectively. The simplest case for chiral OXA–Ru complexes, where the complex possesses symmetric bridging and identical terminal units, is shown in Figure 3 with *meso* ($\Delta\Lambda$) and two enantiomeric isomers ($\Delta\Delta$, $\Lambda\Lambda$). However, by lowering the symmetry in this system through altering the substituents on the bridging and terminal units, it is possible to have a large number of

(7) Measurement was made on a Bruker SMART 1K CCD diffractometer with graphite monochromated Mo K α (0.71073 Å) radiation. Data were collected at the temperature 207(2) K, and the structure was solved by direct methods and expanded using Fourier techniques using SHELXTL. All non-hydrogen atoms were refined anisotropically. Hydrogen atoms were included in idealized positions and not refined. Data were merged and corrected for beam inhomogeneous and absorption using SADSAB. Crystal size: 0.52 \times 0.44 \times 0.20 mm. Monoclinic, *P2₁/n*. Cell dimensions *a* = 11.413(3) Å; *b* = 12.631(3) Å; *c* = 22.655(5) Å; α = 90°; β = 95.192(4)°; γ = 90°. *V* = 3252.6(13) Å³, θ_{max} = 26.02°, ρ = 1.502 g/cm³; *R*₁ = 0.0930 (for reflections with *I* > 2 σ (*I*)), *wR*₂ = 0.1559 (for all reflections).

(8) (a) Balzani, V.; Juris, A. *Coord. Chem. Rev.* **2001**, *211*, 97. (b) Furue, M.; Ishibashi, M.; Satoh, A.; Oguni, T.; Maruyama, K.; Sumi, K. *Coord. Chem. Rev.* **2000**, *208*, 103. (c) Tyson, D. S.; Luman, C. R.; Zhou, X. L.; Castellano, F. N. *Inorg. Chem.* **2001**, *40*, 4063. (d) Walters, K. A.; Trouillet, L.; Guillerez, S.; Schanze, K. S. *Inorg. Chem.* **2000**, *39*, 5496. (e) Hu, Y. Z.; Tsukiji, S.; Shinkai, S.; Oishi, S.; Hamachi, I. *J. Am. Chem. Soc.* **2000**, *122*, 241. (f) Luo, J.; Reddy, K. B.; Salameh, A. S.; Wishart, J. F.; Isied, S. S. *Inorg. Chem.* **2000**, *39*, 2321. (g) Stemp, E. D. A.; Holmlin, R. E.; Barton, J. K. *Inorg. Chim. Acta* **2000**, *297*, 88. (h) Furue, M.; Maruyama, K.; Kanematsu, Y.; Kushida, T.; Kamachi, M. *Coord. Chem. Rev.* **1994**, *132*, 201.

(9) (a) Patterson, B. T.; Foley, F. M.; Richards, D.; Keene, F. R. *J. Chem. Soc., Dalton Trans.* **2003**, *4*, 709. (b) Keene, F. R. *Chem. Soc. Rev.* **1998**, *27*, 185. (c) Fletcher, N. C.; Junk, P. C.; Reitsma, D. A.; Keene, F. R. *J. Chem. Soc., Dalton Trans.* **1998**, 133. (d) Fletcher, N. C.; Keene, F. R. *J. Chem. Soc., Dalton Trans.* **1999**, 683. (e) Patterson, B. T.; Keene, F. R. *Inorg. Chem.* **1998**, *37*, 645.

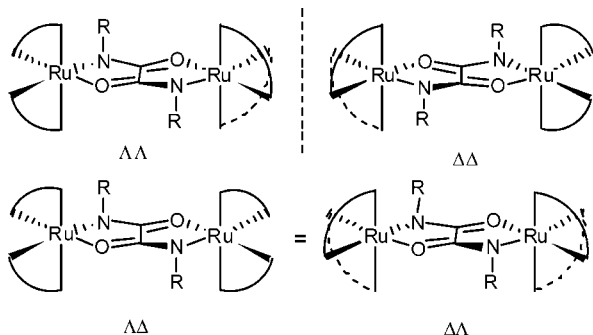


Figure 3. Stereoisomers of symmetric OXA–Ru complexes.

mixtures of diastereomers, enantiomers, geometrical isomers, and even conformational isomers.⁹ Following separation of the *rac* and *meso* forms of an azobis(2-pyridine)-bridged dinuclear ruthenium complex by cation exchange chromatography, it was shown by Keene and co-workers that the ruthenium centers in these systems communicated in unique manners.¹⁰ For example, the MLCT absorptions and redox couples were slightly shifted for the *rac* and *meso* forms of these complexes.

In principle, each diastereomer that is present will also have its own unique NMR spectrum. ¹H and ¹³C NMR analyses of these OXA–Ru complexes did indicate the presence of isomers in solution. For example, the ¹H NMR spectrum of **2e** shows two resonance peaks for the methyl group, one corresponding to the pair of enantiomers and the other to the *meso* compound. For complex **2a**, only one singlet peak for the two methyl groups was observed at 2.15 ppm in the ¹H NMR spectrum, whereas in the ¹³C NMR spectrum there are two peaks at 32.1 and 32.3 ppm for the methyl carbons and two peaks for the carbonyl carbons at 170.7 and 170.8 ppm. Considering the point groups of these systems, it is expected that each diastereomer will provide the 22 resonance peaks in the NMR spectrum. However, due to signal overlapping, only 34 peaks were present in the ¹³C NMR spectrum. For the unsymmetrical complexes, there are at least four stereoisomers present without the *meso* isomer. The ¹³C NMR spectrum of complex **2i** showed two methyl carbons and four distinct carbonyl carbons. By introducing a chiral group into the ligand, the situation becomes even more complicated. For complex **2j**, at least seven distinct sets of resonance peaks were observed in the ¹H and ¹³C NMR spectra. There are significant differences in the resonance intensities, and it is not possible to determine if these are due to overlapping peaks or higher percentages of certain isomers being formed.

Cyclic voltammetry (CV) was utilized to investigate the electrochemical properties of OXA–Ru complexes. Since the isomeric DCH–Ru complexes have been shown to undergo two successive one-electron oxidation steps corresponding to formation of the Ru^{II}/Ru^{III} and Ru^{III}/Ru^{II} states,

(10) Kelso, L. S.; Reitsma, D. A.; Keene, F. R. *Inorg. Chem.* **1996**, *35*, 5144.

Table 1. Electrochemical Data for OXA–Ru Complexes^a

complex	¹ E _{Pa}	¹ E _{Pc}	¹ E _{1/2}	² E _{Pa}	² E _{Pc}	² E _{1/2}	ΔE _{1/2}
2a	533	576	555	961	1033	997	442
2b	659	719	689	901	973	937	248
2c	836	904	870				
2d	513	595	554	708	796	752	198
				881 ^b	971	926	174
2e	599	652	626	1012	1080	1046	420
2f	625	688	657	1035	1103	1069	412
2g	670	745	707	1077	1164	1121	414
2h	527	605	566	918	1014	966	400
2i	601	665	633	1022	1091	1057	424
2j	632	669	651	1061	1125	1093	442

^a Electrochemical data (in mV) are corrected to ferrocene vs SCE.
^b Additional couple due to oxidation of the dimethylaniline group.

it was anticipated that these complexes would behave in an analogous fashion. Indeed, complexes **2a,b,e–j** underwent two reversible oxidation steps as anticipated. The half wave potentials for the first and second oxidation steps range from 555 to 707 mV and 937 to 1121 mV, respectively. In all of these cases, there is a potential window of 400–442 mV between the first and second oxidation steps with the exception of **2b** where the difference is only 248 mV. For complex **2c** without substitutions on the nitrogen atoms, there was only one oxidation step observed. The electrochemical data for OXA–Ru complexes is summarized in Table 1. Figure 4 shows the cyclic voltammogram of complex **2i** with

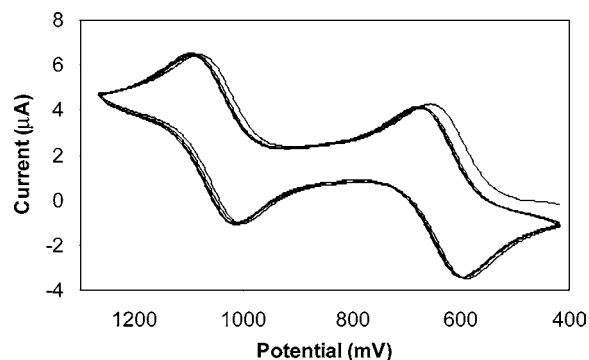


Figure 4. Cyclic voltammogram of **2i** in acetonitrile containing 0.1 M TBAP using a 50 mV/s scan rate (five cycles).

reversible redox cycles over time, indicating that it would be suitable for use as an electrochemical switch.

The spectroelectrochemical properties of the complexes were also examined in order to determine whether the OXA–Ru systems possessed similar electrochromic properties as the DCH–Ru complexes. Figure 5 shows the UV/vis–NIR spectra of complex **2f**. The spectra were recorded using an OTTLE cell by applying different potentials. Complexes in the Ru^{II}/Ru^{II} state display two intense absorptions around 370 and 506 nm associated with the MLCT transitions.

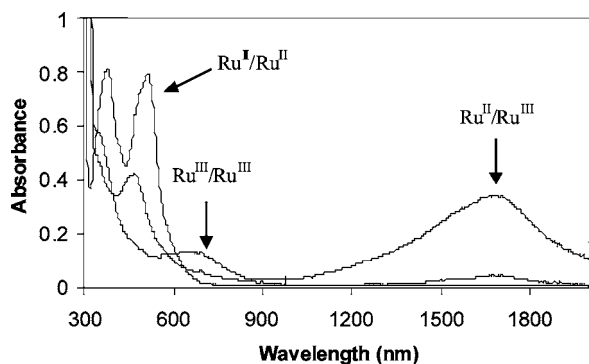


Figure 5. UV/vis–NIR spectra of **2f** in three different oxidation states in acetonitrile containing 0.1 M TBAPF₆.

Oxidation to the Ru^{II}/Ru^{III} state results in the appearance of a strong and broad IVCT band centered in the NIR region. Complex **2b** had the most blue-shifted NIR absorption with the λ_{max} at 1393 nm, followed by complex **2d** at 1474 nm. The rest of the complexes exhibited λ_{max} values around 1650 nm. Upon further oxidation to the Ru^{III}/Ru^{III} state, the intense NIR absorptions disappear and broad peaks appear around 700 nm. At this time, the complexes also precipitated in the OTTLE cell in acetonitrile solutions. These results are in contrast to the DCH–Ru complexes in which a distinct peak typically appeared at 800 nm when the complexes were oxidized to the Ru^{III}/Ru^{III} states. These peaks were assigned to LMCT transitions, which manifest differently in the OXA–Ru complexes. Interestingly, complex **2c**, which showed only one oxidation step by CV, did not show any NIR absorptions upon oxidation in the OTTLE cell. This indicates that the two ruthenium centers were oxidized at the same potential, and therefore a mixed-valence complex was not produced. Thus, hydrogen as the substituents on the nitrogen atoms of the oxamide group results in loss of communication between the metal centers.

The chiroptical properties of ligand **1j** and complex **2j** were examined using circular dichroism (CD) in acetonitrile (Figure 6). The ligand bearing one chiral center exhibited

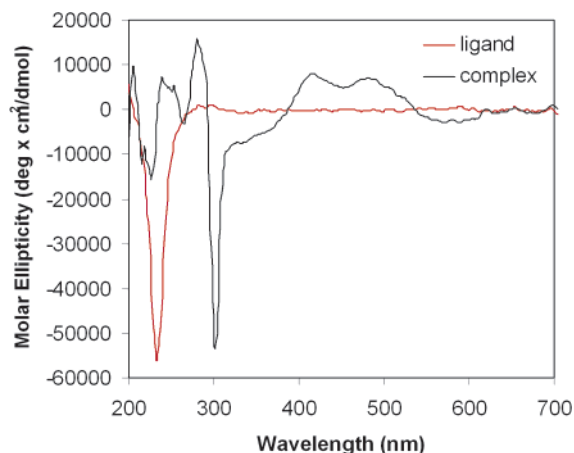


Figure 6. CD spectra of **1j** and **2j** in acetonitrile

one intense negative peak at 234 nm with a molar ellipticity of $-56115 \text{ deg cm}^2 \text{ dmol}^{-1}$. Complex **2j** has its most intense peak at 302 nm with a molar ellipticity of $-53500 \text{ deg cm}^2 \text{ dmol}^{-1}$.

The other enantiomers of ligand **1j** and complex **2j** were also synthesized using (*R*)- α -methylbenzylamine and, as expected, possessed CD spectra that were opposite in sign to those shown in Figure 6.

In summary, the OXA–Ru complexes are a new class of NIR electrochromic compounds, which are useful for studying the electron-transfer process and for potential applications in NIR optical attenuation and chiroptical switching.

Acknowledgment. We thank the Natural Sciences and Engineering Research Council of Canada for financial support.

Supporting Information Available: General synthetic procedure, ¹H and ¹³C NMR spectra of complexes, and a CIF file of the crystal structure of complex **2f**. This material is available free of charge via the Internet at <http://pubs.acs.org>.

OL048021B